ISIJ International, Vol. 44 (2004), No. 6, pp. 1072–1078

The Influence of Solute Carbon in Cold-rolled Steels on Shear Band Formation and Recrystallization Texture

Mark Denis NAVE, Matthew Robert BARNETT and Hossein BELADI

School of Engineering and Technology, Deakin University, Pigdons Road, Geelong, Vic. 3217, Australia.
E-mail: mnave@deakin.edu.au

(*Received on October 27, 2003; accepted in final form on March 5, 2004*)

Two experiments were conducted to clarify the roles of grain size, solute carbon and strain in determining the recrystallization textures of cold-rolled and annealed steels. In the first experiment, samples of coarse-grained low-carbon (LC) and interstitial-free (IF) steels were cold-rolled to a 75 % reduction in thickness. One sample from each steel was polished and cold-rolled an additional 5 %, while the remaining samples were annealed for various times at 650°C. In the second experiment, three samples from a commercial LC steel sheet were rolled 70 % at 300°C. Two of the samples were given a further rolling reduction of 5 % of the original thickness, with one of the samples being given this additional reduction at 300°C and the other at room temperature. Goss recrystallization textures are strengthened by coarse initial grain sizes, the presence of solute carbon and rolling at a temperature where dynamic strain ageing occurs, but are weakened by additional rolling beyond a reduction of 70 %, especially when this extra rolling is conducted at a temperature where dynamic strain ageing does not occur. Characterization of key features of the deformed and recrystallized steels using optical microscopy, scanning electron microscopy (SEM) and electron back-scatter diffraction (EBSD) supports a rationale for these effects based on the repeated activation and deactivation of shear bands and the influence of solute carbon and dynamic strain ageing on the operating life of the bands and the accumulation of strain within them.

KEY WORDS: steel; low-carbon (LC) steel; interstitial-free (IF) steel; cold-rolling; recrystallization; texture; shear bands; Goss; electron back-scatter diffraction (EBSD).

1. Introduction

The recrystallization textures of cold-rolled and annealed steels strongly influence their mechanical and electrical properties. A strong, even ⟨111⟩//ND-fibre texture provides planar and normal anisotropies favourable for deep-drawing, while textures with significant Goss components are detrimental to formability.[1] In contrast, strong Goss or Cube textures facilitate magnetisation and are preferred for electrical steels.[1] Improved understanding of the mechanisms controlling the formation of Goss recrystallization textures is required in order to optimise the properties of steels for each of these applications.

Goss recrystallization textures are promoted by coarse initial grain sizes[2] and high amounts of solute carbon.[3] Shear bands within {111}⟨112⟩ grains are the main sources of Goss nuclei in cold-rolled steels and both shear bands and Goss nuclei form readily in {111}⟨112⟩ single crystals and {111}⟨112⟩ grains within coarse-grained poly-crystals.[2,4,5] The formation of shear bands is favoured by increasing the amount of solute carbon[6,7] and rolling at temperatures where dynamic strain ageing occurs.[8] Recent work[9] indicates that both a sufficient level of solute carbon and a sufficiently coarse grain size are required to generate a Goss recrystallization texture. Furthermore, the strength of the Goss component has been shown to be a complex function of strain, increasing with cold-rolling reduction up to 70 % (true strain=1.2), but reducing with further strain.[3] While the overall effects of grain size, solute carbon and strain on the formation of Goss recrystallization textures are known, the mechanisms that cause these effects are not fully understood.

2. Experimental Procedure

This paper presents results from two experiments conducted to clarify certain aspects of the mechanisms by which grain size, solute carbon and strain influence the formation of Goss recrystallization textures in cold-rolled and annealed steels. The first experiment was conducted on a coarse-grained LC steel (Sample A in **Table 1**) and a coarse-grained Ti-stabilized IF steel (Sample B in Table 1) to clarify the role of solute carbon in coarse-grained steel. Some initial results from this work have been published elsewhere.[10] The second experiment was conducted to further clarify the role of solute carbon by investigating the effect of a small amount of additional rolling at room temperature on the recrystallization texture of a low-carbon steel of commercial grain size (17 μm) that already had been rolled to a moderately-high reduction at 300°C. These temperatures were chosen because reasonably high levels of shear banding would be expected at 300°C due to dynamic strain ageing (DSA), whereas less shear banding would be expected at room temperature.[11–13] Samples C, D and E are

Table 1. Compositions and initial grain sizes of the steels.

Sample	Description	Composition (wt%)					Initial Grain Size (μm)
		C	Ti	Mn	Al	N	
A	CG LC	0.06	0.00	0.2	0.4	0.004	105
B	CG IF	0.003	0.07	0.2	0.02	0.002	160
C, D, E	Comm. LC	0.05	0.00	0.3	0.04	0.003*	17

*Nominal (not measured)

identical in composition and initial grain size (Table 1), having been cut from the same piece of commercial-grade LC steel, but are identified separately due to differences in their subsequent processing.

2.1. Coarse-grained LC and IF Steel

The compositions and initial grain sizes of the coarse-grained LC and IF steels (Samples A and B, respectively) are given in Table 1. The steels were cold-rolled to 75% reduction and annealed for various times at 650°C in a fluid bed furnace. Specimens were prepared in the cold-rolled state and after annealing for various times, including fully-recrystallized specimens. Optical microscopy was performed on etched RD-ND sections of the two steels in the 75% cold-rolled state to characterise the degree of the shear band formation in each steel. The proportion of moderately-to-severely banded grains in each sample was measured by point-counting on a grid. The nature of the shear bands in each steel was characterised in greater detail using back-scattered electron imaging on unetched specimens in the scanning electron microscope. In order to allow an assessment of the quantity and nature of the shear bands still operating at high rolling reductions, the RD-ND face of a 75% cold-rolled sample of each steel was polished and the samples were rolled to reduce their thickness by a further 5% of the original thickness. The proportion of moderately-to-severely banded grains in each sample was measured by point-counting on a grid and the nature of the bands was characterised by optical microscopy. Macro-textures of the specimens in the cold-rolled state were measured by X-ray diffraction (XRD). Macro- and micro-textures of fully- and partially-recrystallized specimens were obtained using electron back-scattered diffraction (EBSD) in a field emission gun scanning electron microscope (FEG-SEM). Rockwell B hardness measurements were used to obtain percent recrystallized versus time data for sample A. Similar data was obtained for sample B from optical micrographs using grid point counting and a sigmoidal curve was fitted to each set of data.

2.2. Commercial LC Steel Rolled at 300°C and Room Temperature

Figure 1(a) shows the processing routes of the samples, together with the points at which deformed (C_{Def}, D_{Def}, E_{Def}) and fully-recrystallized (C_{Rex}, D_{Rex}, E_{Rex}) specimens were extracted. Figure 1(b) shows the details of each stage of the process. All samples were given a pre-heat treatment to ensure that they were in the fully-annealed state prior to rolling and to maximize the amount of carbon in solid solution. Next, all of the samples were rolled at 300°C to a 70% reduction in thickness in three passes. Two of the three samples were rolled to a further 5% reduction on the original thickness, one of these at 300°C (Sample D) and the other at room temperature (Sample E). To ensure the processing of all three samples was as similar as possible (except for the different rolling temperatures and reductions), the precipitation treatment was given to all three samples, although its main purpose was to ensure that as much carbon as possible was precipitated in Sample E prior to the final room temperature rolling step. Macro-textures of the deformed specimens were measured by XRD, while macro-textures of the fully-recrystallized specimens were obtained using EBSD in a FEG-SEM.

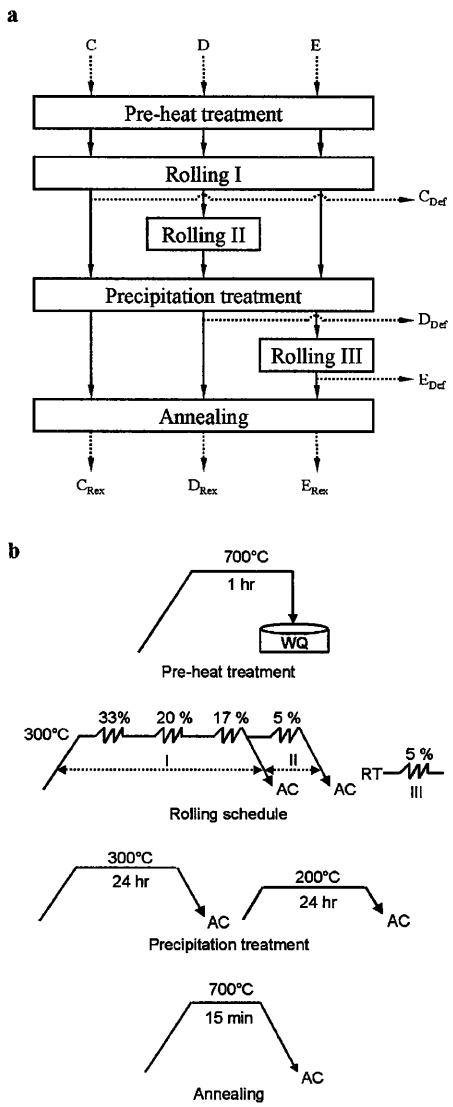

Fig. 1. (a) Processing routes and (b) processing details for samples C, D and E (RT=room temperature, WQ=water quench, AC=air cool).

3. Results

3.1. Coarse-grained LC and IF Steel

Macro-textures for the two coarse-grained steels in the

cold-rolled state are shown in **Fig. 2**. The differences between the two textures are minor. The texture of the IF steel is a little stronger, with higher intensities along the ⟨011⟩//RD- and ⟨111⟩//ND-fibres and spreads towards the cube and {110}⟨110⟩ orientations above 1x random.

Microstructural analysis of etched RD-ND sections of samples in the cold-rolled state showed large amounts of shear bands in both steels (**Fig. 3**), with 60% of the microstructure being moderately-to-severely banded in the IF steel versus 50% in the LC steel. Although grain boundary displacements associated with the bands can be identified in Fig. 3, these displacements are much clearer in the samples that were rolled an additional 5% after polishing, which are discussed in the following paragraph. Backscattered electron images of shear bands and possible shear bands in the two different steels are shown in **Fig. 4**. Other researchers

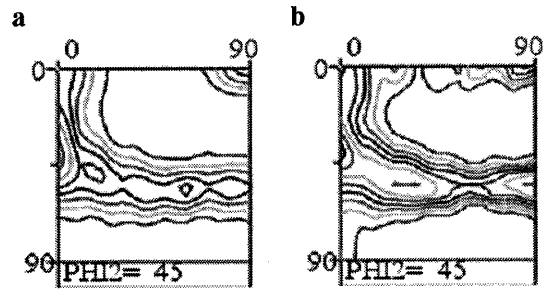

Fig. 2. Orientation distribution functions (φ_2=45° sections with levels 1, 2, 3,..., 8) for samples A (coarse-grained LC steel) and B (coarse-grained IF steel) in the deformed state.

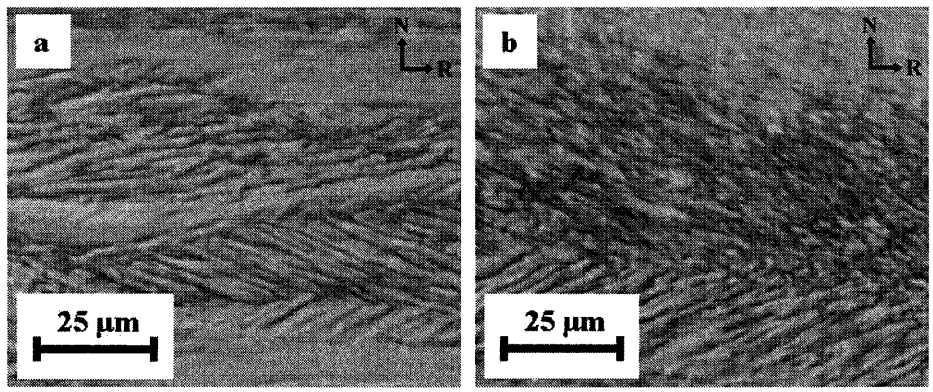

Fig. 3. Optical micrographs of etched RD-ND sections of (a) Sample A (coarse-grained LC steel) and (b) Sample B (coarse-grained IF steel). Reproduced from[10] courtesy of *Materials Science Forum*.

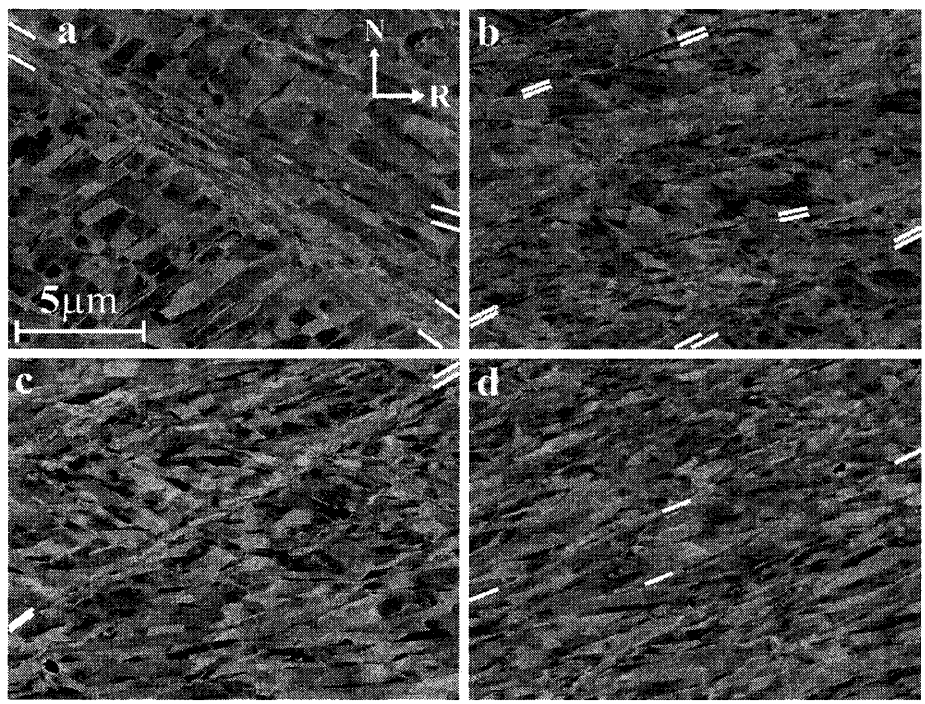

Fig. 4. Backscattered electron images of shear bands and possible shear bands in (a) a near-{110}⟨110⟩ grain and (b) a near-{111}⟨112⟩ grain in sample A: coarse-grained LC steel; (c) a near-{112}⟨112⟩ grain and (d) a near-{111}⟨112⟩ grain in sample B: coarse-grained IF steel. The locations and widths of some of the bands are indicated with short white lines. Each micrograph has the same scale and orientation with respect to the sample coordinate system, as indicated on the top-left micrograph (a).

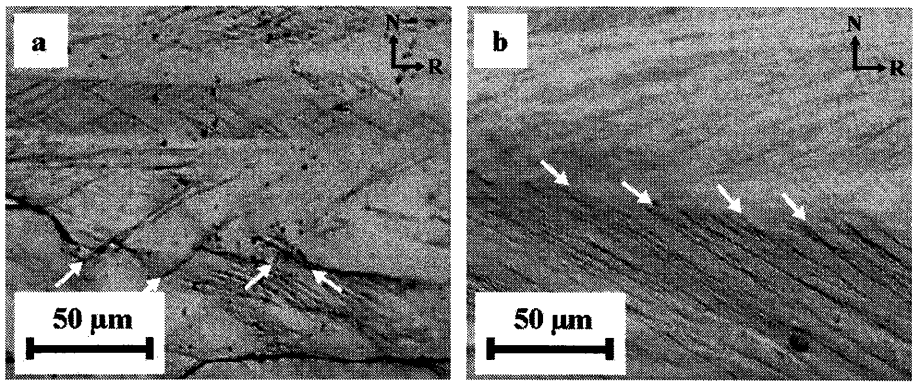

Fig. 5. RD-ND faces of (a) sample A: coarse-grained LC steel and (b) sample B: coarse-grained IF steel. The contours are a result of deformation during a further 5% rolling reduction after the faces of the specimens were polished. Some displacements of the grain boundaries associated with shear bands are marked with white arrows. Reproduced from[10] courtesy of *Materials Science Forum*.

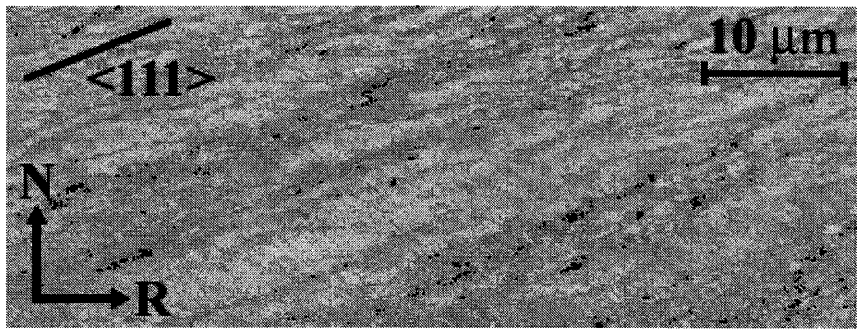

Fig. 6. Part of a {111}⟨112⟩ grain in Sample A (coarse-grained LC steel) showing orientations within 15° of the ideal Goss orientation in black. The ⟨111⟩ direction of the {111}⟨112⟩ grain that lies in the RD-ND plane and is approximately parallel to the shear bands (and lines of Goss orientations) is marked as well. The image background consists of a grey-scale orientation map showing up to 15° deviation from the ideal {111}⟨112⟩ orientation superimposed on a grey-scale Kikuchi band contrast map, both digitally-brightened.

have observed similar microstructures and arrangements of bands in cold-rolled[6,7] and warm-rolled steels.[14] In some grains (*e.g.* Figs. 4(a), 4(c)), the shear bands clearly cut across a microstructure that consists of cells aligned in microbands. These bands are considered shear bands since there are distinct displacements of the microband structures parallel to the shear bands from one side of the shear bands to the other. In other grains, (*e.g.* Figs. 4(b), 4(d)), the cell structures and microbands were much less distinct and were crossed by sets of approximately parallel but slightly wavy lines. While the microstructures between the pairs of lines are distinctly different to those outside them, it is quite difficult to establish whether the bands have carried localized shear and thus to classify them as shear bands with conviction.

Optical microscopy on the (un-etched) polished surfaces of the specimens that were cold-rolled an additional 5% revealed a higher proportion of moderately-to-severely banded material in the LC steel (40%) compared with the IF steel (30%). Furthermore, the deformation appeared to be more heavily localized in the LC steel, than the IF steel. An example of this is shown in **Fig. 5**, where a set of shear bands in the LC steel has caused grain boundary displacements of approximately 20 μm (Fig. 5(a)), while the grain boundary displacements associated with the shear bands in the IF steel are approximately 5 μm (Fig. 5(b)). These bands can confidently be classified as shear bands due to the significant, discrete displacements of the grain boundaries where they are intersected by the bands.

High-resolution orientation maps (0.15 μm pixel spacing) collected on a {111}⟨112⟩ grain in each steel revealed a marked difference in the frequency of near-Goss orientations within the grains. The {111}⟨112⟩ grain in the coarse-grained LC steel, contained a significant proportion of near-Goss orientations, located along lines of heavily-localized deformation (**Fig. 6**). In contrast, hardly any near-Goss orientations were present in the {111}⟨112⟩ grain in the coarse-grained IF steel. Point-to-point misorientation profiles were measured in the {111}⟨112⟩ grain in each steel along five lines, each 15 mm long and parallel to the sample rolling direction. The combined results for the five lines on each steel are presented in **Fig. 7**. While the {111}⟨112⟩ grains in both steels exhibit a reasonably high degree of orientational fragmentation, the grain in the LC steel contained a higher proportion of high-angle (>15°) boundaries. Being measured on only a single {111}⟨112⟩ grain for each steel, these results should be treated with caution. However, it may be noted that the higher degree of fragmentation in the LC steel is consistent with the more heavily-localized flow in the LC steel than the IF steel in the samples that were cold-rolled an additional 5% (Fig. 5).

Recrystallization occurs much more rapidly in the LC

steel (90% complete within 2 min) compared with the IF steel (90% complete in approximately 100 min), as shown in **Fig. 8**. In the fully-recrystallized state, there are strong differences between the macro-textures of the two samples (**Fig. 9**). The IF steel displays a strong ND-fibre with peaks near the {111}⟨112⟩ orientations, whereas in the LC steel the ND-fibre is much weaker and the texture is dominated by the Goss orientation.

3.2. Commercial LC Steel Rolled at 300°C and Room Temperature

The bulk textures of samples C to E in the deformed state are shown in **Fig. 10**. The textures are typical of cold-rolled steels and the differences between them are very minor. There is a slight strengthening of the texture with the additional 5% rolling and this strengthening is more marked in the sample rolled the additional 5% at room temperature (compare Fig. 10(c) with Fig. 10(a)) than in the sample rolled the additional 5% at 300°C (compare Fig. 10(b) with Fig. 10(a)).

The bulk textures of samples C, D and E in the fully-recrystallized state are shown in **Fig. 11**. The texture of sample C (CR75% at 300°C) consists of an ND-fibre with stronger intensities near the {111}⟨112⟩ orientations than

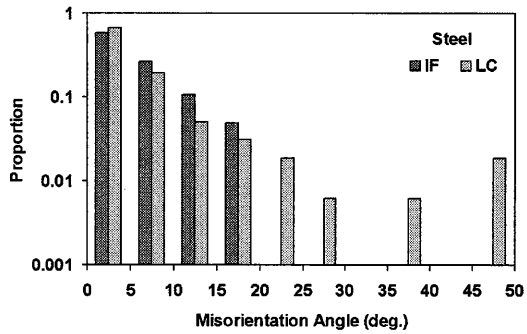

Fig. 7. Misorientation angle distributions for {111}⟨112⟩ grains in the coarse-grained LC and IF steels.

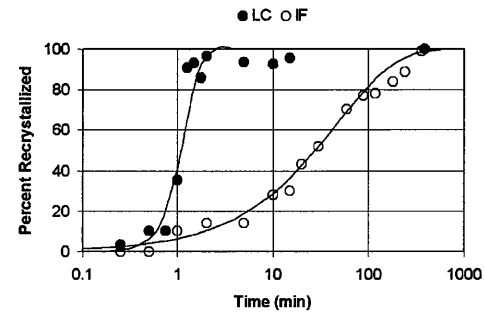

Fig. 8. Percent recrystallised versus time for samples A (coarse-grained LC) and B (coarse-grained IF).

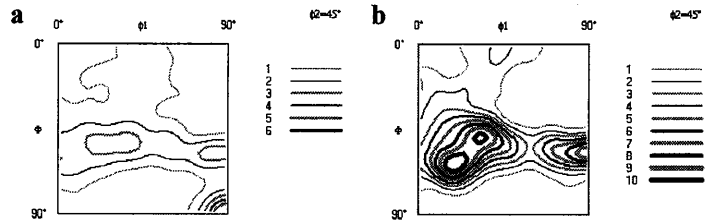

Fig. 9. Orientation distribution functions (φ_2=45° sections) for (a) sample A: coarse-grained LC and (b) sample B: coarse-grained IF in the fully-recrystallised state.

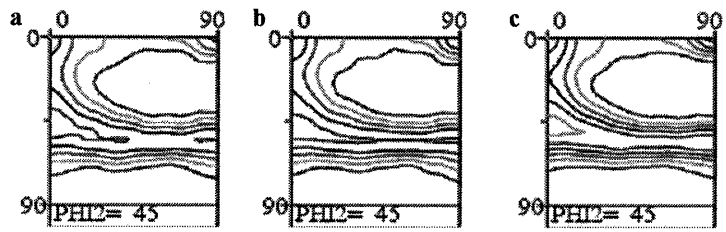

Fig. 10. Orientation distribution functions (φ_2=45° sections with levels 1, 2, 3,..., 8) for (a) sample C (CR 70% at 300°C), (b) sample D (CR 75% at 300°C) and (c) sample E (CR 75%, with 70% at 300°C and 5% at room temperature), in the deformed state.

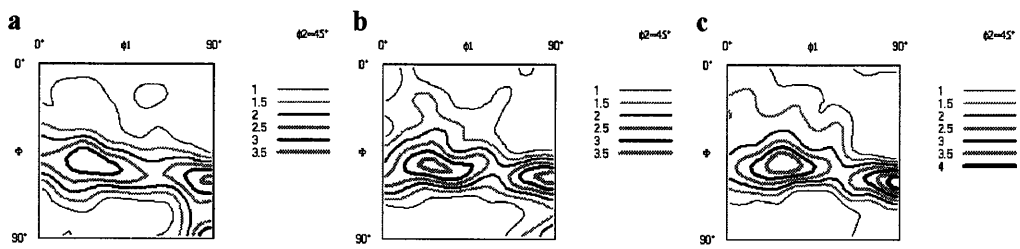

Fig. 11. Orientation distribution functions (φ_2=45° sections) for (a) sample C (CR70% at 300°C), (b) sample D (CR75% at 300°C) and (c) sample E (CR75% with the first 70% at 300°C and the final 5% at room temperature), in the fully-recrystallized state.

the {111}⟨110⟩ orientations, plus strong intensities near the {110}⟨001⟩, or Goss, orientation. Sample D (CR75% at 300°C) has a similar texture although the intensities near the Goss orientation are somewhat weaker and those near {111}⟨112⟩ are just slightly stronger. In sample E (CR75%, with 70% at 300°C and 5% at room temperature) the intensities near {111}⟨112⟩ are slightly stronger than in either samples C or D and the intensities near the Goss orientation are considerably weaker than for sample D and much weaker than for sample C.

4. Discussion

The results of the experiments conducted on the coarse-grained LC and IF steels clearly demonstrate that Goss recrystallization textures do not form in IF steel with a coarse initial grain size, but do form in coarse-grained LC steel (Fig. 9). This is the case despite the two different grades of steel having relatively similar deformation textures (Fig. 2). These two results confirm earlier work by Lesne *et al.*[9] The results presented in this paper indicate that the difference in recrystallization texture arises from a much higher frequency of Goss nuclei at shear bands in the cold-rolled LC steel (Fig. 6). Although the shear bands in the two steels are present in reasonably similar proportions and have similar morphologies (Figs. 3, 4), a smaller proportion of shear bands are still operating at high rolling reductions in the IF steel and the deformation is not as strongly localized in the IF steel as it is in the LC steel (Figs. 5, 7). These results provide a basis for understanding the relative scarcity of Goss nuclei within the cold-rolled microstructure of the coarse-grained IF steel, as discussed in more detail below.

The results from the experiments conducted on the (much finer-grained) commercial LC steel show that a recrystallization texture with a substantial Goss component can be generated by rolling to a reduction of 70% at 300°C, but that the strength of the Goss component decreases a small amount with additional rolling at 300°C and much more markedly with additional rolling at room temperature (Fig. 11). As in the experiment involving the coarse-grained steels, this substantial difference in recrystallization texture occurs despite very little difference between the cold-rolled textures of the steels (Fig. 10). The reduction in the intensity of the Goss component of the recrystallization texture with additional rolling is consistent with the work of Schlippenbach and Lücke[3] that showed the Goss component to decrease with additional rolling at room temperature beyond a reduction of 70%. However, the results presented in this paper demonstrate that the decrease in the Goss component of the recrystallization texture at high rolling reductions is sensitive to the rolling temperature. In a steel that has been rolled at a temperature where dynamic strain ageing occurs (in this case, 300°C), there is only a small reduction in the intensity of the Goss component when additional rolling is carried out in the dynamic strain ageing region, but a much larger reduction when the additional rolling is performed outside this region (in this case, at room temperature).

It is known[4,5] (and confirmed in this work, Fig. 6) that Goss nuclei form predominantly in shear bands within {111}⟨112⟩ grains. Also, it is known that shear banding is promoted by coarse grain sizes[4] and the presence of solute carbon,[6–8] for rolling temperatures between 0 and 400°C.[8] Consequently, it would be easy to rationalize the relative prevalence of Goss nuclei in LC steels that have coarse initial grain sizes or are rolled temperatures where dynamic strain ageing occurs simply on the basis of an increased amount of shear banding. However, the relatively similar proportion of shear-banded material in the coarse-grained LC and IF steels, together with the substantial reduction in the Goss component achieved in the commercial LC steel rolled an additional 5% at room temperature following a 70% reduction at 300°C, indicates that the situation is more complex than this.

The results presented in this paper can be rationalized on the basis of the following two reasonable assumptions. The first assumption is that shear bands, once formed, do not operate continuously for the remainder of the deformation, but have a finite life. The finite life of shear bands has been demonstrated in cold-rolled brass[15] and it has been suggested that the continual activation and deactivation of shear bands plays a key role in the orientational fragmentation of ND-fibre grains in cold- and warm-rolled steels.[16,17] The second assumption is that the shear band life is longer in the LC steel than in the IF grade. This can be justified on the basis that the presence of solute carbon in the LC steel leads to a low rate sensitivity of the flow stress, which favours flow localization.[11–13] Some experimental support for this assumption is provided by the observation that approximately 80% of the shear bands evident in the LC steel following the rolling reduction of 75% were re-activated during the subsequent 5% rolling reduction. For the IF steel, only half of the bands were reactivated.

Given the assumption of shear bands that are repeatedly forming, carrying shear and ceasing to operate, the results presented in this paper can be rationalized as follows. Crystal plasticity theory predicts that material within a shear band in a {111}⟨112⟩ grain will rotate towards Goss while the band is carrying shear,[4,5,16] but will tend to rotate back towards {111}⟨112⟩ under plane-strain deformation[18] once the shear band ceases to operate. If it is assumed that shear bands that form in coarse-grained IF steel have a shorter life-span (and therefore carry less strain over their life) than those that form in coarse-grained LC steel, then the material within the shear bands in the IF steel will not rotate as far away from {111}⟨112⟩ during operation of the bands and will not require as much subsequent deformation to rotate back close to {111}⟨112⟩ once the bands cease to operate. As a corollary, it is assumed that the shear bands in the LC steel operate for longer and carry more strain over their life. Consequently, the material within these bands rotates further towards the Goss orientation during operation of the shear bands and requires more subsequent deformation to rotate back near to {111}⟨112⟩ once the shear bands cease to operate. It should be noted that, as the shear bands operate and the material within the bands rotates towards the Goss orientation, the crystal rotation rate will initially decrease with strain before increasing again once the material has rotated past a critical orientation (a pseudo-stable orientation in shear).[5,16] If the shear bands within the coarse-grained LC steel operate for a longer period of time, then more material within the bands is likely to be rotated

beyond this point of pseudo-stability, where the rate of rotation towards the Goss orientation becomes more rapid.

This mechanism is consistent with the results of the second experiment, which demonstrated that a recrystallization texture with a strong Goss component is formed, even in a relatively fine-grained LC steel, when rolling is carried out at a temperature where dynamic strain ageing occurs. At this temperature, the shear bands are more likely to operate for a longer period of time because dynamic strain ageing gives rise to low, and even negative, rate sensitivities, which favour flow localization.[11–13] Consequently, it is more likely that material within the bands will rotate to near-Goss orientations. When additional rolling is carried out at room temperature, where dynamic strain ageing does not occur, less shear bands are activated. The material within the shear bands that are not reactivated is rotated back away from the Goss orientation, leading to a much weaker Goss component in the recrystallization texture.

5. Conclusions

The following conclusions can be made regarding the formation of shear bands and Goss recrystallization textures in steels and the influence of solute carbon and dynamic strain ageing on their formation.

(1) Goss recrystallization textures are formed as a result of the nucleation of Goss grains at shear bands within deformed grains having orientations near $\{111\}\langle 112\rangle$.

(2) Relatively few Goss orientations are generated within shear bands in $\{111\}\langle 112\rangle$ grains in interstitial-free steels, even when these steels have a coarse initial grain size, so Goss recrystallization textures do not develop in these steels.

(3) In low-carbon steels, the generation of Goss within shear bands in near-$\{111\}\langle 112\rangle$ grains is more prevalent when the steels have a coarse initial grain size or are rolled at temperatures where dynamic strain ageing occurs. The Goss component of the recrystallization texture is strengthened as a result.

(4) Goss-oriented material generated in shear bands in low-carbon steel by rolling at a temperature where dynamic strain ageing occurs may be rotated back away from the Goss orientation by additional rolling at a temperature where dynamic strain ageing does not occur. This results in a substantial reduction in the intensity of the Goss component in the recrystallization texture.

(5) At high rolling reductions, localization of flow is more severe in coarse-grained low-carbon steel than in coarse-grained interstitial-free steel and a higher proportion of shear bands are still operating at high rolling reductions in coarse-grained low-carbon steel.

(6) The results support the view that the enhanced generation of Goss nuclei in shear bands when sufficient solute carbon is present during rolling, and particularly when rolling is conducted at a temperature where dynamic strain ageing occurs, is a result of the increased period of operation of the shear bands and the increased accumulation of strain within the bands under these conditions.

Acknowledgments

The authors would like to acknowledge the Australian Research Council (ARC) for funding this work and Leo Kestens for X-ray diffraction measurement of the textures of the deformed steels.

REFERENCES

1) F. J. Humphreys and M. Hatherly: Recrystallization and Related Annealing Phenomena, Pergamon, Oxford, (1995), 400, 408 and 411.
2) M. Abe, Y. Kokabu, Y. Hayashi and S. Hayami: *Trans. Jpn. Inst. Met.*, **23** (1982), 718.
3) U. V. Schlippenbach and K. Lüke: Proc. of 8th Int. Conf. on Textures of Materials—ICOTOM 8, ed. by J. S. Kallend and G. Gottstein, TMS, Warrendale, PA, (1988), 861.
4) T. Haratani, W. B. Hutchinson, I. L. Dillamore and P. Bate: *Met. Sci.*, **18** (1984), 57.
5) K. Ushioda and W. B. Hutchinson: *ISIJ Int.*, **29** (1989), 862.
6) H. Inagaki: *Z. Metallkd.*, **81** (1990), 474.
7) M.-Y. Huh, D. Raabe and O. Engler: *Steel Res.*, **66** (1995), 353.
8) M. R. Barnett and J. J. Jonas: *ISIJ Int.*, **37** (1997), 697.
9) L. Lesne, H. Réglé, C. Maurice and J. H. Driver: Proc. of 21st Risø Int. Symp. on Materials Science, ed. by N. Hansen *et al.*, Risø National Laboratory, Roskilde, Denmark, (2000), 407.
10) M. D. Nave and M. R. Barnett: *Mater. Sci. Forum*, **408–412** (2002), 907.
11) J. D. Baird: *Metall. Rev.*, **16** (1971), 1.
12) A. K. Taheri, T. M. Maccagno and J. J. Jonas: *ISIJ Int.*, **35** (1995), 1532.
13) M. R. Barnett and J. J. Jonas: *ISIJ Int.*, **39** (1999), 856.
14) M. Z. Quadir and B. J. Duggan: *Mater. Sci. Forum*, **426–432** (2003), 3769.
15) B. J. Duggan, M. Hatherly, W. B. Hutchinson and P. T. Wakefield: *Met. Sci.*, **12** (1978), 343.
16) M. R. Barnett: *ISIJ Int.*, **38** (1998), 78.
17) B. Hutchinson and P. Bate: Proc. of IF Steels 2003, ISIJ, Tokyo, (2003), 337.
18) J. J. Jonas, L. Kestens and A. O. Humphreys: Proc. of IF Steels 2003, ISIJ, Tokyo, (2003), 393.